Appl Microbiol Biotechnol (2016) 100:3989–3998
DOI 10.1007/s00253-015-7224-7

Replacing a piece of loop-structure in the substrate-binding groove of *Aspergillus usamii* β-mannanase, AuMan5A, to improve its enzymatic properties by rational design

Yun Hai Dong[1] · Jian Fang Li[1] · Die Hu[2] · Xin Yin[2] · Chun Juan Wang[1] · Shi Han Tang[1] · Min Chen Wu[3]

Received: 6 August 2015 / Revised: 12 November 2015 / Accepted: 5 December 2015 / Published online: 17 December 2015

Abstract To perfect the enzymatic properties of AuMan5A, a mesophilic glycoside hydrolase (GH) family 5 β-mannanase from *Aspergillus usamii*, its loop-structure substitution was carried out by rational design and followed by megaprimer PCR. Based on the structural analysis and enzymatic property comparison of various β-mannanases, a piece of loop-structure with seven amino acids between two β-strands (βD and βE) in the substrate-binding groove, named "Loop DE," was speculated to be correlative to the thermostability and catalytic efficiency of GH family 5 β-mannanases. Therefore, three AuMan5A's mutants, AuMan5A-Af, AuMan5A-An, and AuMan5A-Th, were designed by substituting a Loop DE sequence (^{316}KSPDGGN^{322}) of AuMan5A with the corresponding sequences of other three family 5 β-mannanases, respectively. Then, the mutant-encoding genes, *Auman5A-Af*, *Auman5A-An*, and *Auman5A-Th*, were constructed as designed theoretically and then expressed in *Pichia pastoris* GS115. The expressed recombinant AuMan5A-Af (re-AuMan5A-Af) displayed the temperature optimum (T_{opt}) of 75 °C, T_m value of 76.6 °C and half-life ($t_{1/2}$) of 480 min at 70 °C, which were 10 and 12.1 °C higher and 48-fold longer than those of re-AuMan5A, respectively. Its catalytic efficiency (k_{cat}/K_m) was 12.7-fold that of re-AuMan5A. What is more, the site-directed mutagenesis of D320G in AuMan5A-Af was performed. The T_{opt} and $t_{1/2}$ of expressed re-AuMan5A-Af^{D320G} decreased to 70 °C and 40 min, respectively, while its k_{cat}/K_m was only 35 % of that of re-AuMan5A-Af. These results demonstrated that the mutation of G320 (in AuMan5A) into D320 (in AuMan5A-Af) through Loop DE substitution was mainly responsible for the thermostability and catalytic efficiency improvement of AuMan5A-Af.

Keywords Loop-structure substitution · Rational design · β-Mannanase · Thermostability · Catalytic efficiency

Yun Hai Dong and Jian Fang Li contributed equally to this work.

Electronic supplementary material The online version of this article (doi:10.1007/s00253-015-7224-7) contains supplementary material, which is available to authorized users.

✉ Min Chen Wu
biowmc@126.com

[1] State Key Laboratory of Food Science and Technology, School of Food Science and Technology, Jiangnan University, 1800 Lihu Road, Wuxi 214122, China

[2] Key Laboratory of Carbohydrate Chemistry and Biotechnology, Ministry of Education, School of Biotechnology, Jiangnan University, 1800 Lihu Road, Wuxi 214122, China

[3] Wuxi Medical School, Jiangnan University, 1800 Lihu Road, Wuxi 214122, China

Introduction

Mannan, after xylan, is the second most abundant hemicellulose in nature. The complete degradation of mannan requires the synergistic action of mannolytic enzymes. Among them, β-mannanase (endo-β-1,4-D-mannanase, EC 3.2.1.78) is a key enzyme in that it cleaves the internal β-1,4-D-mannosidic linkages of mannan backbone, yielding manno-oligosaccharides (Chauhan et al. 2012; Dhawan and Kaur 2007). Based on the primary structure alignment and hydrophobic cluster analysis, almost all known β-mannanases have been classified into glycoside hydrolase (GH) families 5, 26, and 113 (http://www.cazy.org/fam/acc_GH.html). Analysis of three-dimensional (3-D) structures displayed that all β-mannanases in the three families belong to GH clan-A (Zhang et al. 2008). The clan-A enzymes share the triose phosphate isomerase (TIM) $(\beta/\alpha)_8$ barrel fold and two

absolutely conserved glutamate residues at the C-termini of β4 and β7 which act as the general acid/base and nucleophile, respectively, to cleave glycosidic bonds via a double displacement mechanism with the retention of anomeric configuration (van Zyl et al. 2010). Some β-mannanase crystal structures from bacteria, fungi, and plants have been resolved, revealing an open and hydrophobic cleft where the β-1,4-D-mannosidic linkages of mannan backbone insert and get cleaved (Chauhan et al. 2012; Dilokpimol et al. 2011). β-Mannanases possess great potential in industrial processes, such as animal feed, baking, coffee extraction, and pulp bleaching (Moreira and Filho 2008). However, the broad applications of most commercialized β-mannanases were limited by their low catalytic activity, weak substrate affinity, and/or poor tolerance to extreme environments (Li et al. 2014).

The thermostability, catalytic efficiency, and substrate affinity of β-mannanases are considered as the most important enzymatic properties for their applicability in industrial bioprocesses. To meet the increasing demands for β-mannanases with superior properties, more interests are being focused on modifying their primary and/or 3-D structures by means of directed evolution and rational design (Couturier et al. 2013a; Huang et al. 2014). To date, some researches about β-mannanase modifications, such as the fusion of a carbohydrate-binding module into the N- or C-terminus of a catalytic domain and the site-directed mutagenesis of crucial amino acids in the substrate-binding groove (SBG), have been conducted to improve their substrate affinity and/or thermostability (Li et al. 2014; Tang et al. 2013). However, few studies have been reported on the substitution of loop-structures in SBG of β-mannanases to improve their enzymatic properties.

Several studies have demonstrated that the modification of the loop-structures in close vicinity to the active centers of glycoside hydrolases could improve their thermostability and/or catalytic efficiency (Cheng et al. 2012; Duan et al. 2013; Voutilainen et al. 2010). In our previous researches, an AuMan5A-encoding gene, *Auman5A* (GenBank accession no. HQ839639), was cloned from *Aspergillus usamii* YL-01-78 and analyzed (Tang et al. 2011). In this work, to improve the thermostability and catalytic efficiency of a wild-type AuMan5A, three mutants, AuMan5A-Af, AuMan5A-An, and AuMan5A-Th, were designed by replacing a Loop DE of AuMan5A with the corresponding ones of other family 5 β-mannanases from *Aspergillus fumigatus*, *Aspergillus nidulans*, and *Trichoderma harzianum*, respectively. Then, three mutant-encoding genes, *Auman5A-Af*, *Auman5A-An*, and *Auman5A-Th*, were constructed by megaprimer PCR as designed theoretically and expressed in *Pichia pastoris* GS115. The pH and temperature properties and catalytic efficiency of recombinant β-mannanases, re-AuMan5A, re-AuMan5A-Af, re-AuMan5A-An, and re-AuMan5A-Th, were determined and compared. In addition, the mechanism on the thermostability and catalytic efficiency improvement of re-AuMan5A-Af was preliminarily analyzed by site-directed mutagenesis. To our knowledge, this is the first report on the substitution of AuMan5A's Loop DE to improve its thermostability and catalytic efficiency by rational design.

Materials and methods

Strains, vectors, and culture media

Escherichia coli JM109 and vector pUCm-T (Sangon, Shanghai, China) were used for gene cloning and DNA sequencing. The recombinant T-vector, pUCm-T-*Auman5A*, was constructed and preserved in our laboratory (Tang et al. 2011). *E. coli* DH5α and vector pPICZαA (Invitrogen, San Diego, CA, USA) were applied for the construction of recombinant expression vectors, while *Pichia pastoris* GS115 (Invitrogen, USA) was used for the expression of genes. All culture media were prepared as described in the instruction of the EasySelect™ *Pichia* Expression Kit (Invitrogen, USA).

Evolutionary analysis of β-mannanases

Using AuMan5A as the template, the homology search at NCBI website (http://www.ncbi.nlm.nih.gov/) for other GH family 5 β-mannanase primary structures, which shared more than 50 % identity with that of AuMan5A, was performed using the BLAST server. A total of 167 family 5 β-mannanase primary structures were searched out for evolutionary analysis. The homology alignment between or among β-mannanases was accomplished using a DNAMAN 6.0 software or ClustalW2 program (http://www.ebi.ac.uk/Tools/msa/clustalw2/).

Homology modeling and rational design of AuMan5A's mutants

The known crystal structures of GH family 5 β-mannanases, having high sequence identity with AuMan5A, from *Aspergillus niger* (PDB code: 3WH9) (Huang et al. 2014), *Podospora anserina* (3ZIZ) (Couturier et al. 2013b) and *Trichoderma reesei* (1QNR) (Sabini et al. 2000) were used as the templates for homology modeling. The 3-D structures of AuMan5A and its mutants were modeled with the multiple template-based technique using the SALIGN program (http://salilab.org/DBAli/?page=tools_&action=f_salign) and the MODELLER 9.11 program (http://salilab.org/modeller/). In this work, the OE1 of the nucleophile Glu276 in AuMan5A was defined as the center of SBG. All amino acids of AuMan5A in proximity to the OE1 within 15 Å were located using a PyMol software (http://pymol.org/), and their frequencies were generated through multiple alignment among 167 β-mannanase sequences. The residue whose

frequency was below 70 % and was considered as non-conserved, and used as the candidate for site-directed mutagenesis. Based on the above structural analysis and comparison of enzymatic properties, a piece of loop-structure with seven residues between two β-strands (βD and βE) in SBG, designated Loop DE, was speculated to be correlative to the GH family 5 β-mannanase properties. Therefore, three AuMan5A's mutants were designed by replacing a Loop DE (^{316}KSPDGGN^{322}) of AuMan5A with the corresponding ones of other three family 5 β-mannanases, respectively.

Construction of the mutant β-mannanase genes

The genes, *Auman5A-Af*, *Auman5A-An*, and *Auman5A-Th*, were constructed by replacing a DNA fragment (21 bp in length) encoding a Loop DE of *Auman5A* with the corresponding ones, respectively, using the megaprimer PCR method (Xie and Shi 2009). PCR primers were designed according to the nucleotide sequence of *Auman5A* and DNA fragments encoding the Loop DEs of β-mannanases from *A. fumigatus*, *A. nidulans,* and *T. harzianum*, and synthesized by Sangon as listed in Table S1. The gene fragment, *AfmR*, *AnmR,* or *ThmR*, was first amplified from pUCm-T-*Auman5A* with a forward primer Af-F, An-F, or Th-F and a reverse primer Man5A-R as the following conditions: a denaturation at 94 °C for 3 min and 30 cycles at 94 °C for 30 s, 55 °C for 30 s, and 72 °C for 10 s. Then, using pUCm-T-*Auman5A* as the template again, the second-round PCR for the complete mutant gene, *Auman5A-Af*, *Auman5A-An*, or *Auman5A-Th*, was carried out with primers Man5A-F and *AfmR*, *AnmR*, or *ThmR* under the same conditions, except for an elongation at 72 °C for 75 s in 30 cycles. The target PCR products were gel-purified and inserted into vector pUCm-T, followed by transforming them into *E. coli* JM109, respectively. The recombinant T-vectors, named pUCm-T-*Auman5A-Af*, pUCm-T-*Auman5A-An*, and pUCm-T-*Auman5A-Th*, were confirmed by DNA sequencing.

Expression and purification of the recombinant β-mannanases

The *Auman5A* and its mutant genes were excised from their respective recombinant T-vectors with *Eco*RI and *Not*I, and inserted into the vector pPICZαA digested with the same enzymes. Then, the recombinant expression vectors, pPICZαA-*Auman5A*, pPICZαA-*Auman5A-Af*, pPICZαA-*Auman5A-An*, and pPICZαA-*Auman5A-Th*, were separately linearized with *Sal*I, and electroporated into *Pichia pastoris* GS115. *Pichia pastoris* transformants were inoculated on a YPDS plate containing zeocin at 400 μg mL^{-1} for screening multiple copies of four integrated β-mannanase genes, respectively. *Pichia pastoris* GS115 transformed with pPICZαA was used as the negative control (*Pichia pastoris* GSC). The expression of β-mannanase gene in *Pichia pastoris* GS115 was performed according to the instruction of EasySelect^{TM} *Pichia* Expression Kit with slight modification (Li et al. 2012). After the *Pichia pastoris* transformant was induced by 1 % (*v/v*) methanol at 30 °C for 96 h, the expressed recombinant β-mannanase was purified to homogeneity according to the method as reported previously (Tang et al. 2013).

Enzyme activity and protein assays

β-Mannanase activity was assayed with the 3,5-dinitrosalicylic acid (DNS) method (Li et al. 2014). One unit (U) of β-mannanase activity was defined as the amount of enzyme liberating 1 μmol of reducing sugar equivalent per minute from locust bean gum (Sigma, St. Louis, MO, USA) under the assay conditions (at pH 3.6 and 65 °C for 10 min). The protein content was measured with the BCA-200 Protein Assay Kit (Pierce, Rockford, IL, USA), using bovine serum albumin as the standard. The sodium dodecyl sulfate-polyacrylamide gel electrophoresis (SDS-PAGE) was performed according to the method of Laemmli (1970) on a 12.5 % gel. The isolated proteins were visualized by staining with Coomassie Brilliant Blue R-250 (Sigma, USA), whose molecular weights were estimated using a Quantity One software based on the standard marker proteins.

Enzymatic properties of the recombinant β-mannanases

The pH optimum and stability of the purified recombinant AuMan5A or its mutant were determined according to the method as reported previously (Tang et al. 2014). The temperature optimum was measured, at pH optimum, at temperatures ranging from 50 to 80 °C. To evaluate the thermostability, the purified recombinant β-mannanase (without substrate) was incubated at pH optimum and 70 °C for 80 min. The thermal inactivation half-life ($t_{1/2}$) was defined as a time at which the residual β-mannanase activity, measured under the standard assay conditions, retained 50 % of its original activity. The specific activity (U mg^{-1}) of the purified recombinant β-mannanase was measured at its temperature and pH optima with locust bean gum concentrations ranging from 1 to 10 mg mL^{-1}. The specific activity versus the substrate concentration was plotted to verify whether the hydrolytic mode of the recombinant β-mannanase conforms to the Michaelis–Menten equation. The K_m and k_{cat} values were determined by non-linear regression analysis using an Origin 9.0 software. All data were expressed as the mean ± standard deviation (SD) from the three independent experiments or parallel measurements.

Measurement of the melting temperature

The melting temperature (T_m) is defined as a temperature, at which half of a protein's 3-D structure is unfolded. Any

protein with high T_m value means it has a high thermostability (Jang et al. 2010). In this work, the T_m value was measured with the protein thermal shift (PTS) method, using a PTS Kit (Applied Biosystems, Carlsbad, CA, USA) and a LightCycler 480 II real-time PCR apparatus (Roche, Basel, Switzerland). A brief protocol was as follows: the purified recombinant β-mannanase was mixed with fluorescence dye and placed into a 96-well PCR plate, followed by heating from 50 to 95 °C at an elevated rate of 1 °C min^{-1}, while deionized water instead of β-mannanase was used as the control. The excitation and emission wavelengths were 533 and 640 nm, respectively. Three replicates were conducted independently. The T_m value was considered as a temperature corresponding to the peak of a derivative melting curve, which was plotted using the 'T_m calling' method.

Site-directed mutagenesis of the residue in AuMan5A-Af

To validate whether the mutation of G320 (in AuMan5A) into D320 (in AuMan5A-Af) through substitution of a Loop DE was mainly responsible for the thermostability and catalytic efficiency improvement, the site-directed mutagenesis of D320G in AuMan5A-Af was designed. An AuMan5A-Af^{D320G}-encoding gene, *Auman5A-Af*^{D320G}, was constructed by megaprimer PCR as mentioned earlier, and expressed in *Pichia pastoris* GS115. The expressed re-AuMan5A-Af^{D320G} was purified and characterized.

Results

Selection of a piece of loop-structure in SBG of AuMan5A

Based on the analysis of the modeled 3-D structure of AuMan5A by a PyMol software, 112 amino acid residues of AuMan5A, in close proximity to the OE1 of nucleophile Glu276 within 15 Å, were located (Fig. 1a, b). Those residues sit in SBG of AuMan5A, which may be correlative to its enzymatic properties. To eliminate the conserved amino acid residues, the frequencies of 112 residues which were analyzed by multiple alignment were summarized in Fig. S1. In this work, a total of 35 residues with frequencies lower than 70 % were regarded as the non-conserved ones. Among them, a group of six continuous residues (^{317}SPDGGN^{322}) was selected, which composed a piece of loop-structure in SBG of AuMan5A.

Rational design of AuMan5A's mutants

It has been demonstrated that when amino acid residues or partial structures are changed, enzymes tend to lose their activities or alter their properties in many cases (Choi et al. 2012). To confirm a piece of loop-structure in SBG of AuMan5A to be used for substitution, we selected 14 GH family 5 fungal β-mannanases whose primary structures shared more than 50 % identity with that of AuMan5A and whose crystal structures and enzymatic properties were reported. The multiple alignment of their partial primary structures were performed (Fig. 2) and their enzymatic properties were summarized in Table 1.

The modeled 3-D structure of AuMan5A displayed that a piece of loop-structure in SBG with six residues (^{317}SPDGGN^{322}) belongs to a big surface loop (W306 − G327) which was defined as the loop 8 in β-mannanase (Couturier et al. 2013b), connecting the last β-sheet and α-helix at the C-terminus. The loop 8 consists of two

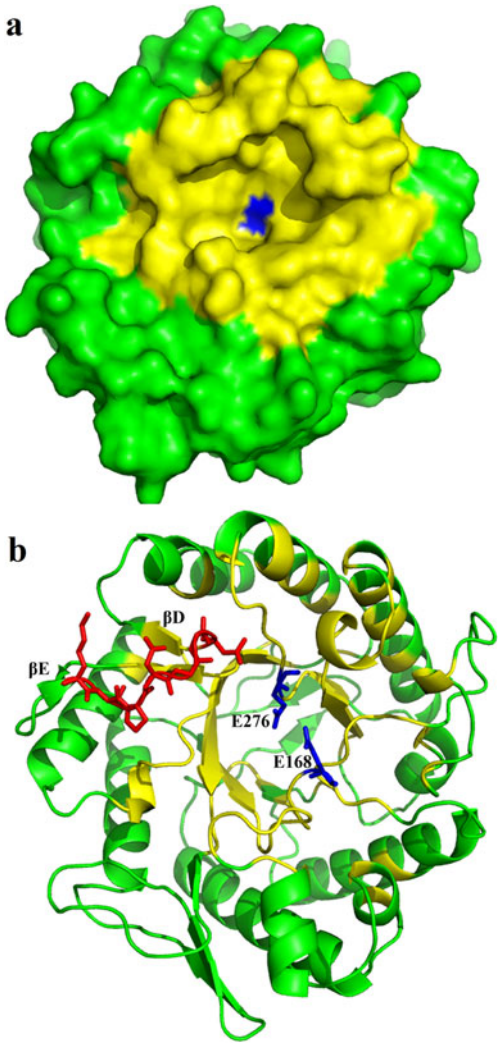

Fig. 1 The modeled 3-D structure of AuMan5A. **a** Surface view of AuMan5A. One of the two catalytic glutamate residues, E276, acts as the nucleophile and is colored in *blue*. The residues in proximity to the OE1 of E276 within 15 Å are colored in *yellow*. **b** Cartoon view of AuMan5A. The two catalytic residues, E168 and E276, are shown in *blue sticks*. Loop DE consisted of seven residues and is shown in *red sticks*

Fig. 2 Multiple alignment of the C-terminal amino acids sequences of some fungal GH family 5 β-mannanases. Loop DEs are *boxed*. GenBank accession numbers are indicated on the *right side*

anti-parallel β-strands (βD and βE) (Sabini et al. 2000) and one short loop-structure with seven residues between βD and βE (Loop DE). Based on the result of multiple alignment, the Loop DE sequences vary greatly in fungal family 5 β-mannanases (Fig. 2), which were classified into four groups according to their similarity with that of AuMana5A (Table 1). From each group, we selected one representative β-mannanase with outstanding properties. Man I and ThMan5A separately from *A. fumigatus* and *T. harzianum* in groups 2 and 4 possess the excellent catalytic efficiencies (k_{cat}/K_m), while Man5XZ3 from *A. nidulans* in group 3 has the high temperature optimum (T_{opt}). Thus, the three Loop DE sequences of fungal β-mannanases from *A. fumigatus* (PSPNDHF), *A. nidulans* (QTHNDGN), and *T. harzianum* (AQSNSDPY) were selected for replacing that (KSPDGGN) of AuMan5A, respectively, forming three mutants AuMan5A-Af, AuMan5A-An, and AuMan5A-Th.

Table 1 Loop DE sequences and some enzymatic properties of different fungal GH family 5 β-mannanases sharing identity more than 50 % with AuMan5A

Group	Origin	Enzyme	Identity[a] (%)	Loop DE sequence	T_{opt} (°C)	pH_{opt}	SA[c] (U mg^{-1})	k_{cat}[c] (s^{-1})	k_{cat}/K_m[c] (mL mg^{-1} s^{-1})	Reference
1	*Aspergillus usamii*	AuMan5A	100	KSPDGGN	65	3.5–4.0	338	409	227	This work
	Aspergillus niger	ManBK[b]	98	KSPDDGN	80	4.5	2570	330	165	Do et al. 2009; 3WH9
	Aspergillus niger	AnMan5A	98	KSPDDGN	70	3.5	221.8	231.1	210.1	Li et al. 2012
	Aspergillus sulphureus	AsMan5A	94	ESPDDGN	50	2.4	366	276	297	Chen et al. 2007
	Aspergillus aculeatus	rec-Man	74	QSPNDGN	75	2.5–3.0	138	213	177	Pham et al. 2010
	Aspergillus nidulans	ManA	69	PSPDDGN	NR[d]	NR[d]	NR[d]	NR[d]	NR[d]	Dilokpimol et al. 2011
	Talaromyces trachyspermus	TtMan5A[b]	67	QSPNDGY	NR[d]	NR[d]	NR[d]	NR[d]	NR[d]	3WFL
	Penicillium pinophilum	rMan5C1	63	QSPNDGN	70	4.0	1035	NR[d]	NR[d]	Cai et al. 2011b
	Penicillium	Man5C6	57	KSADDGN	70	4.5	226	1800	146	Cai et al. 2011a
2	*Aspergillus fumigatus*	Man I	61	PSPNDHF	60	4.5	562	1935	630	Puchart et al. 2004
3	*Aspergillus nidulans*	Man5XZ3	67	QTHNDGN	80	5.0	171	190	173	Lu et al. 2014
	Thielavia arenaria	Man5XZ7	61	QTHNDGH	75	5.0	704	511	96	Lu et al. 2013
	Podospora anserina	PaMan5A[b]	61	QTHNDGF	60	4.0	68	70	15	Couturier et al. 2011; 3ZIZ
4	*Trichoderma harzianum*	ThMan5A	58	AQSNSDPY	70	5.5	1544	3083	771	Wang et al. 2014
	Trichoderma reesei	TrMan5A[b]	56	AQSNSDPY	70	3.0–4.0	86	NR[d]	NR[d]	Stålbrand et al. 1993; 1QNR

[a] The identity of primary structure with AuMna5A

[b] The 3-D structure of the proteins have been determined

[c] Specific activity, K_m and k_{cat}/K_m for locust bean gum as the substrate

[d] Not reported

Expression and purification of the recombinant β-mannanases

A total of 80 multicopy *Pichia pastoris* transformants, containing four kinds of β-mannanase genes, were picked out on a YPDS plate with 400 μg mL^{-1} zeocin for flask expression tests. Among all transformants tested, four strains, labeled as *Pichia pastoris* GSAuM, GSAuM-Af, GSAuM-An, and GSAuM-Th, expressing the highest re-AuMan5A, re-AuMan5A-Af, re-AuMan5A-An, and re-AuMan5A-Th activities, respectively, were screened and applied for subsequent studies. No β-mannanase activity was detected in the cultured supernatant of the negative control (*Pichia pastoris* GSC) under the same expression conditions.

Four recombinant β-mannanases were separately purified to homogeneity by a combination of ammonium sulfate precipitation, ultrafiltration and Sephadex G-75 gel chromatography. SDS-PAGE analysis of the purified re-AuMan5A, re-AuMan5A-Af, re-AuMan5A-An, or re-AuMan5A-Th displayed one single protein band with an apparent molecular weight of about 50.0 kDa (Fig. 3, lanes 2–5). Their specific activities towards 5 mg mL^{-1} locust bean gum under the standard assay conditions were 406, 3630, 1420, and 3140 U mg^{-1}, respectively. The specific activities of re-AuMan5A-Af, re-AuMan5A-An, and re-AuMan5A-Th displayed 8.9-, 3.5-, and 7.7-fold higher than that of re-AuMan5A, respectively.

pH and temperature characteristics of the recombinant β-mannanases

The re-AuMan5A or re-AuMan5A-An exhibited the highest activity at a pH range of 3.5–4.0. The pH optimum of re-AuMan5A-Af was at pH 3.0–4.0, while pH optima of re-AuMan5A-Th showed two pH ranges of 3.5–4.0 and 5.0–5.5, respectively (Fig. 4). Incubated at 40 °C for 60 min at varied pH values (2.5–7.5), four recombinant β-mannanases

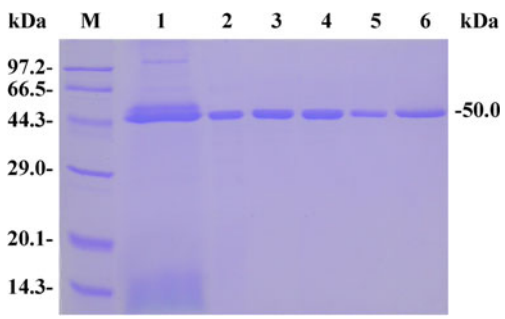

Fig. 3 SDS-PAGE analysis of re-AuMan5A and its mutants. Lane *M*, standard protein molecular mass markers; lane *1*, the cultured supernatant of the transformant expressing re-AuMan5A; lanes *2–6*, re-AuMan5A, re-AuMan5A-Af, re-AuMan5A-An, re-AuMan5A-Th, and re-AuMan5A-Af^{D320G}, purified from the cultured supernatants, respectively

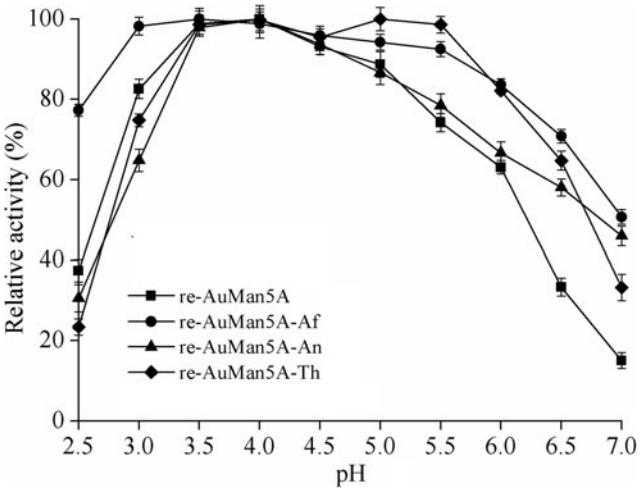

Fig. 4 Effects of pH on activity of re-AuMan5A and its mutants. pH optima of the enzymes were determined, respectively, at 65 °C in buffers of pH ranging from 2.5 to 7.0. Each value in the panel represents the mean ± SD ($n = 3$)

retained more than 90 % of their original activities at a pH range of 3.0–7.0 (data not shown). The temperature optimum of re-AuMan5A was 65 °C similar to that of re-AuMan5A-An, whereas the temperature optima of re-AuMan5A-Af and re-AuMan5A-Th were 75 and 70 °C, respectively (Fig. 5a). Incubated at their respective pH optima and at 70 °C for 80 min, the thermal inactivation half-life ($t_{1/2}$) of re-AuMan5A was 10 min (Fig. 5b), while those of re-AuMan5A-Af (incubated at 70 °C until 10 h) and re-AuMan5A-Th were 480 and 25 min, respectively, which were 48- and 2.5-fold longer than that of re-AuMan5A. However, the half-life of re-AuMan5A-An decreased to 5 min.

The emission intensity of the fluorescence dye combined with hydrophobic regions of a protein increased gradually as the protein was unfolding at the high temperature (Niesen et al. 2007). Based on this mechanism, the T_m values of re-AuMan5A, re-AuMan5A-Af, re-AuMan5A-An, and re-AuMan5A-Th were determined to be 64.5, 76.6, 63.2, and 69.1 °C, respectively, corresponding to the peak values of their derivative melting curves (Fig. 6). The T_m values of four recombinant β-mannanases corresponded to their thermostability levels (Fig. 5b).

Kinetic parameters of the recombinant β-mannanases

The K_m and k_{cat} values of the four recombinant enzymes towards LBG were determined and summarized in Table 2. The findings indicate that all enzymes exhibited normal Michaelise-Menten kinetics. Compared with re-AuMan5A, the apparent K_m values of three mutants, re-AuMan5A-Af, re-AuMan5A-An, and re-AuMan5A-Th, decreased by 22, 44, and 37 %, respectively. In addition, the catalytic constants of all the mutants were significantly enhanced. As shown in Table 1, re-AuMan5A-Af, re-AuMan5A-An, and re-

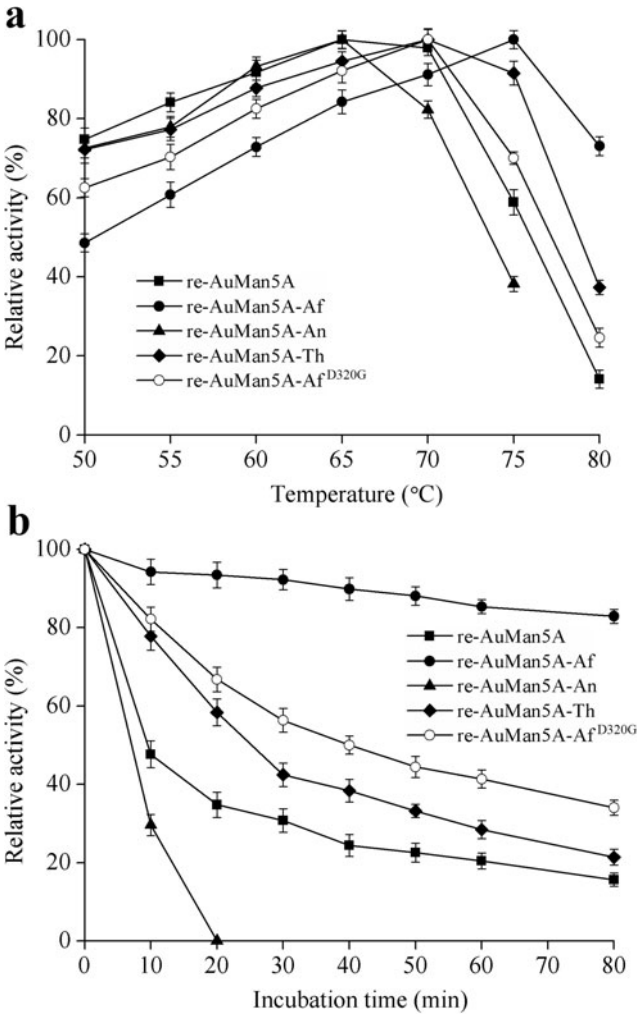

Fig. 5 Effects of temperature on activity (**a**) and stability (**b**) of re-AuMan5A and its mutants. Temperature optima of the enzymes were determined, respectively, in buffer of pH 3.6 and at temperatures ranging from 50 to 80 °C. Their half-lives were assayed, respectively, by incubating them in buffer of pH 3.6 at 70 °C in different time, and the residual enzyme activities were measured under the standard assay conditions. Each value in the panel represents the mean ± SD ($n = 3$)

AuMan5A-Th displayed 9.9-, 3.4-, and 6.9-fold increases in k_{cat} values as compared to the wild-type. Consequently, the catalytic efficiencies (k_{cat}/K_m) of re-AuMan5A-Af, re-AuMan5A-An, and re-AuMan5A-Th were 12.7-, 6.0- and 11.0-fold that of re-AuMan5A.

Characterization of re-AuMan5A-Af^{D320G}

The recombinant single-site mutant of re-AuMan5A-Af, re-AuMan5A-Af^{D320G}, displayed the same molecular weight (50.0 kDa) as the four enzymes on SDS-PAGE (Fig. 3, lane 6). The specific activity of re-AuMan5A-Af^{D320G} was 1080 U mg^{-1}, displaying a significant decrease compared with re-AuMan5A-Af. Re-AuMan5A-Af^{D320G} had the similar pH profile with re-AuMan5A-Af (data not shown). The

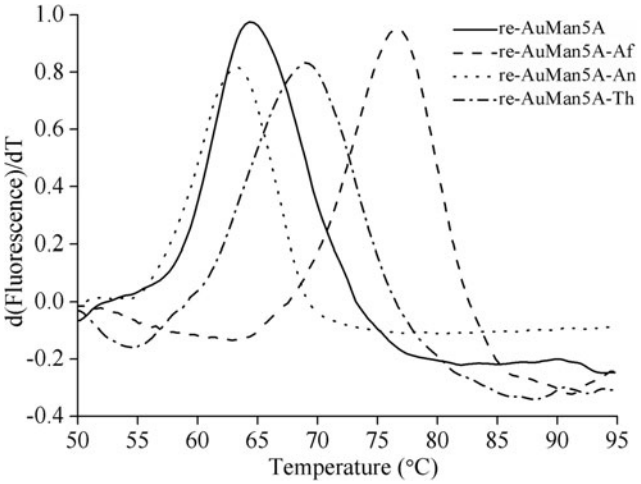

Fig. 6 Derivative melting curves of re-AuMan5A and its mutants. The emission intensity of the fluorescence dye was recorded from 50 to 95 °C at an elevated rate of 1 °C min^{-1}

temperature optima and half-life at 70 °C of the mutant were 70 °C and 40 min (Fig. 4a), respectively, lower and shorter than those of re-AuMan5A-Af. Re-AuMan5A-Af^{D320G} was subjected to kinetic analysis at its temperature optimum of 70 °C (Table 2). The K_m and k_{cat} values were both lower than those of re-AuMan5A-Af. Particularly, the kinetic constant of the mutant was 23 % of that of re-AuMan5A-Af, resulting a significant decrease in catalytic efficiency.

Discussion

Though all β-mannanases from different GH families share a common $(\beta/\alpha)_8$ barrel fold and perform hydrolysis by the retaining mechanism, the sequence similarities between different families are rather low. Even the most common two subfamilies in family 5, A7 (eukaryotic mannanases) and A8 (bacterial mannanases), share an identity rarely greater than 20 % between them (Hilge et al. 1998; Sabini et al. 2000), making sequence-based analysis within the family challenging. We tried to carry out the multiple sequence alignment within homologous sequences that shared more than 50 % identity with AuMan5A, and thus the conservation at each position can be assessed. Introducing a mutation at a position that is strongly conserved is likely to result in a significant loss of function (Jaouadi et al. 2010), and the strategy of modifying residues surrounding the active site of β-mannanase regardless of their conservation to accelerate the catalytic reaction was rather inefficient (Huang et al. 2014). So, we chose the non-conserved sites in SBG for mutagenesis, keeping away from the critical sites that may be involved in catalytic reaction.

Fungal GH family 5 β-mannanases are generally acidophilic and have pH optima ranging from 1.5 to 6 (Moreira and Filho 2008). Re-AuMan5A has a moderate pH optimum

Table 2 Kinetic parameters of re-AuMan5A and its mutants

Variant	k_{cat} (s^{-1})	K_m (mg mL^{-1})	k_{cat}/K_m (mL mg^{-1} s^{-1})	Fold
re-AuMan5A	409 ± 9	1.80 ± 0.07	226.7	1.0
re-AuMan5A-Af	4050 ± 90	1.41 ± 0.03	2870.0	12.7
re-AuMan5A-An	1380 ± 40	1.00 ± 0.03	1370.8	6.0
re-AuMan5A-Th	2810 ± 20	1.13 ± 0.03	2487.6	11.0
re-AuMan5A-Af ^{D320G}	929 ± 15	1.06 ± 0.04	877.0	3.9

Assays were performed using the purified enzymes at their temperature optima in 50 mM Na_2HPO_4-citric acid buffer of pH 3.6 with locust bean gum concentrations ranging from 1 to 10 mg mL^{-1}. Each value of the results represents the mean ± SD ($n = 3$)

range in this area. Interestingly, the mutant re-AuMan5A-Th has an additional pH optimum range of 5.0–5.5, which is similar to that of its loop sequence donor, pH 5.5 of ThMan5A. Meanwhile, re-AuMan5A-Af has an broadened pH optimum range of 3.0–4.5, which makes the enzyme more efficient in acid environment. It is crucial for enzyme applied in feed and food industries with a high activity in acidic condition (Xu et al. 2013).

The temperature profiles of mutants were all altered compared to that of the wild-type, indicating that Loop DE is an important factor for β-mannanase thermostability. Mobile surface loops have been found to serve as unfolding initiation sites, which allow solvent penetration to the core of the protein leading to unfolding (Voutilainen et al. 2010). Accordingly, we demonstrate the feasibility of improving the thermal stability of β-mannanase by modifying Loop DE or even loop 8.

The increase in temperature optimum of re-AuMan5A-Af is quiet unexpected, since its loop sequence donor Man I from *A. fumigatus* has a low temperature optimum of 60 °C (Table 1). Furthermore, re-AuMan5A-An possesses a decreased temperature optimum of 65 °C, whereas its donor, Man5XZ3 from *A. nidulans*, displays the highest activity at 80 °C. When it comes to re-AuMan5A-Th, its temperature optimum is coincident with that of the donor ThMan5A. It can be concluded that Loop DE is an effective but not the determinant factor for β-mannanase's temperature optimum.

Analysis of the modeled structure showed that when G320 is substituted for D320, AuMan5A-Af is predicted to form three additional hydrogen bonds for the side chain of D320 with other surrounding residues (Fig. 7b), which could not be formed by G320 for no side chain (Fig. 7a). These hydrogen bonds tended to confer reduced flexibility of the loop and thus increasing the thermostability of the protein (Duan et al. 2013). The decreased temperature optimum and shortened half-live of AuMan5A-Af^{D320G} demonstrated that the single mutation had negative effect on the thermostability of AuMan5A-Af, which has proved the above hypothesis. In addition, the substitution of G321H in AuMan5A-Af makes the side chain of residue 321 reach out from the loop-structure. Thus, H321 can approach to T280 and create a new hydrogen bond with it (Fig. 5b). It is well-recognized that when a proline

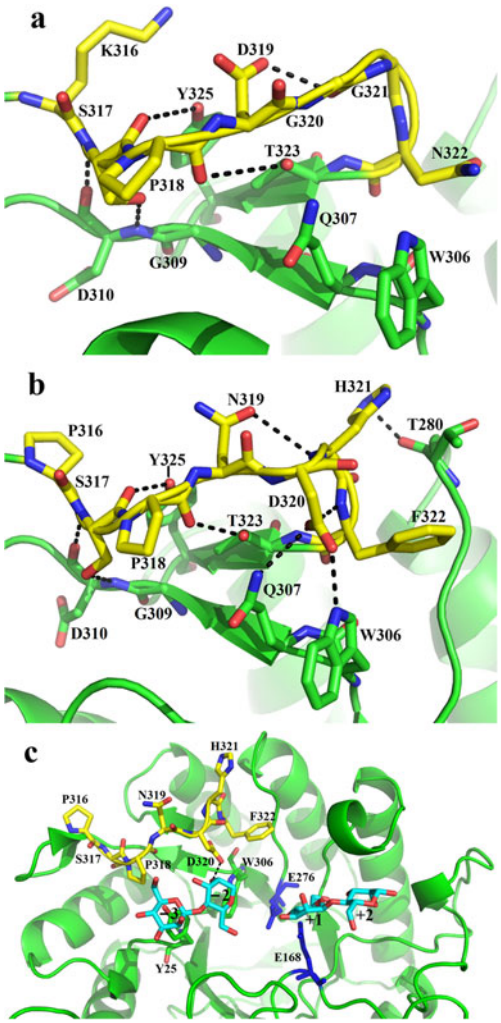

Fig. 7 Structural predictions of hydrogen bonds interactions in AuMan5A and AuMan5A-Af. **a**, **b** Predicted hydrogen bonds interactions between the residues on Loop DE and the surrounding ones in AuMan5A and AuMan5A-Af, respectively. **c** The substrate-biding groove of AuMan5A-Af with mannobioses modeled in subsites −3, −2, +1, and +2. The structures of GH family 5 β-mannanases in complex with mannobioses from *T. fusca* and *T. reesei*, respectively, were superimposed on the top of the structure of PaMan5A to map the substrate-binding subsites −3 to −2 and +1 to +2. Loop DE is adjacent to the subsites and D320 is supposed to make hydrogen bond with OH(2) group of the sugar in subsite −2

residue is introduced in a loop, the proline can rigidify the loop by restricting the number of available main chain conformations (Ghollasi et al. 2013; Xie et al. 2011). In this way, the additional mutation to proline in Loop DE provides extra thermostability for AuMan5A-Af over the wild-type and other mutants. Also, that may partially explain the thermal stability decrease in AuMan5A-An for none proline in its Loop DE. Consequently, the significant increase in thermostability with regard to AuMan5A-Af can be ascribed to four newly introduced hydrogen bonds and an additional mutation to proline after loop substitution.

Analysis of kinetic parameters demonstrated considerable changes in catalytic constants of all mutants compared to re-AuMan5A, suggesting that some significant alterations occurred in catalytic hydrolysis by them. The k_{cat} value of re-AuMan5A-Af is higher than the biggest one of ThMan5A in Table 1. When temperature rises, the catalytic reaction tends to accelerate, so the highest k_{cat} value of re-AuMan5A-Af may be partially concerned with its highest temperature optimum at which the catalytic parameters were determined. But it should be noted that all the enzymes were generally stable under their optimal temperatures except re-AuMan5A-Af, for which re-AuMan5A-Af cannot retain 50 % of its original activity after 10-min incubation at 75 °C (data not shown). We speculate that the catalytic efficiency of AuMan5A-Af will be improved further if it is more stable.

The k_{cat} value of re-AuMan5A-Af^{D320G} is higher than that of the wild-type, but much lower than re-AuMan5A-Af, indicating D320 is one of the critical factors responsible for the increase in turnover of AuMan5A-Af as well as other substitution mutants. From the structure of AuMan5A-Af in complex with mannobiose modeled in subsites −2 and −3, Loop DE is adjacent to the substrate-binding sites of β-mannanase (Fig. 7c). D320 in AuMan5A-Af (D320 in AuMan5A-An and D321 in AuMan5A-Th) was likely to be involved in making hydrogen bond with OH(2) group of the sugar at subsite −2 (corresponding to D321 in TrMan5A) (Sabini et al. 2000; Dilokpimol et al. 2011), whereas G320 in AuMan5A is beyond hydrogen bond forming. The hydrogen bonds between residues and substrate were acknowledged to be important in substrate recognition and binding for enzyme (Sabini et al. 2000), but the Gly-to-Asp change here may have greater influence on product release.

In conclusion, after structural bioinformatics and evolutionary analysis, we generated three mutants of AuMan5A by substituting a piece loop-structure in SBG of AuMan5A with the corresponding sequences of other three fungal family 5 β-mannanases. One of the mutants AuMan5A-Af displayed the highest thermostability, along with an improved pH optimum profile suitable for the industrial use. What is more, this mutant has the significantly improved catalytic efficiency, which is outstanding among fungal GH family 5 β-mannanase. Site-directed mutagenesis of D320G on AuMan5A-Af was preformed, and the results demonstrated that the mutation of G320 to D320 was mainly responsible for the increases in thermal stability and catalytic efficiency of AuMan5A-Af. This work provides an effective strategy for improving multiple functions of β-mannanase and even other enzymes, and further demonstrates that rational design based on structural bioinformatics and evolutionary analysis could be a useful approach to reach optimum enzymes for application purposes.

Acknowledgments The authors are grateful to Prof. Xianzhang Wu (School of Biotechnology, Jiangnan University, Jiangsu, China) for providing technical assistance.

Compliance with ethical standards

Conflict of interest All the authors declare that they have no competing interests.

Funding This work was financially supported by the National Nature Science Foundation of China (No. 31271811), the Fundamental Research Funds for the Central Universities of China (JUSRP51412B) and the Postgraduate Innovation Training Project of Jiangsu, China (KYLX_1170).

Ethical Statement This article does not contain any studies with human participants or animals performed by any of the authors.

References

Cai H, Shi P, Huang H, Luo H, Bai Y, Yang P, Meng K, Yao B (2011a) An acidic β-mannanase from *Penicillium* sp. C6: gene cloning and over-expression in *Pichia pastoris*. World J Microbiol Biotechnol 27:2813–2819

Cai H, Shi P, Luo H, Bai Y, Huang H, Yang P, Yao B (2011b) Acidic β-mannanase from *Penicillium pinophilum* C1: cloning, characterization and assessment of its potential for animal feed application. J Biosci Bioeng 112:551–557

Chauhan PS, Puri N, Sharma P, Gupta N (2012) Mannanases: microbial sources, production, properties and potential biotechnological applications. Appl Microbiol Biotechnol 93:1817–1830

Chen X, Cao Y, Ding Y, Lu W, Li D (2007) Cloning, functional expression and characterization of *Aspergillus sulphureus* β-mannanase in *Pichia pastoris*. J Biotechnol 128:452–461

Cheng YS, Ko TP, Huang JW, Wu TH, Lin CY, Luo W, Li Q, Ma Y, Huang CH, Wang AHJ, Liu JR, Guo RT (2012) Enhanced activity of *Thermotoga maritima* cellulase 12A by mutating a unique surface loop. Appl Microbiol Biotechnol 95:661–669

Choi SH, Kim HS, Lee EY (2012) Multiple sequence alignment-inspired mutagenesis of marine epoxide hydrolase of *Mugil cephalus* for enhancing enantioselective hydrolytic activity. J Ind Eng Chem 18:72–76

Couturier M, Haon M, Coutinho PM, Henrissat B, Lesage-Meessen L, Berrin JG (2011) *Podospora anserina* hemicellulases potentiate the *Trichoderma reesei* secretome for saccharification of lignocellulosic biomass. Appl Environ Microbiol 77:237–246

Couturier M, Feliu J, Bozonnet S, Roussel A, Berrin JG (2013a) Molecular engineering of fungal GH5 and GH26 beta-(1,4)-

mannanases toward improvement of enzyme activity. PLoS One 8: e79800

Couturier M, Roussel A, Rosengren A, Leone P, Stalbrand H, Berrin JG (2013b) Structural and biochemical analyses of glycoside hydrolase families 5 and 26 β-(1,4)-mannanases from *Podospora anserina* reveal differences upon manno-oligosaccharide catalysis. J Biol Chem 288:14624–14635

Dhawan S, Kaur J (2007) Microbial mannanases: an overview of production and applications. Crit Rev Biotechnol 27:197–216

Dilokpimol A, Nakai H, Gotfredsen CH, Baumann MJ, Nakai N, Abou Hachem M, Svensson B (2011) Recombinant production and characterisation of two related GH5 endo-β-1,4-mannanases from *Aspergillus nidulans* FGSC A4 showing distinctly different transglycosylation capacity. Biochim Biophys Acta 1814:1720–1729

Do BC, Dang TT, Berrin JG, Haltrich D, To KA, Sigoillot JC, Yamabhai M (2009) Cloning, expression in *Pichia pastoris*, and characterization of a thermostable GH5 mannan endo-1,4-β-mannosidase from *Aspergillus niger* BK01. Microb Cell Fact 8:59

Duan X, Chen J, Wu J (2013) Improving the thermostability and catalytic efficiency of *Bacillus deramificans* pullulanase by site-sirected mutagenesis. Appl Environ Microbiol 79:4072–4077

Ghollasi M, Ghanbari-Safari M, Khajeh K (2013) Improvement of thermal stability of a mutagenised α-amylase by manipulation of the calcium-binding site. Enzyme Microb Technol 53:406–413

Hilge M, Gloor SM, Rypniewski W, Sauer O (1998) High-resolution native and complex structures of thermostable β-mannanase from *Thermomonospora fusca*-substrate specificity in glycosyl hydrolase family 5. Structure 6:1433–1444

Huang JW, Chen CC, Huang CH, Huang TY, Wu TH, Cheng YS, Ko TP, Lin CY, Liu JR, Guo RT (2014) Improving the specific activity of β-mannanase from *Aspergillus niger* BK01 by structure-based rational design. Biochim Biophys Acta 1844:663–669

Jang MK, Lee SW, Lee DG, Kim NY, Yu KH, Jang HJ, Kim S, Kim A, Lee SH (2010) Enhancement of the thermostability of a recombinant β-agarase, AgaB, from *Zobellia galactanivorans* by random mutagenesis. Biotechnol Lett 32:943–949

Jaouadi B, Aghajari N, Haser R, Bejar S (2010) Enhancement of the thermostability and the catalytic efficiency of *Bacillus pumilus* CBS protease by site-directed mutagenesis. Biochimie 92:360–369

Laemmli UK (1970) Cleavage of structural proteins during the assembly of the head of Bacteriophage T4. Nature 227:680–685

Li JF, Zhao SG, Tang CD, Wang JQ, Wu MC (2012) Cloning and functional expression of an acidophilic β-mannanase gene (Anman5A) from *Aspergillus niger* LW-1 in *Pichia pastoris*. J Agric Food Chem 60:765–773

Li J, Wei X, Tang C, Wang J, Zhao M, Pang Q, Wu M (2014) Directed modification of the *Aspergillus usamii* β-mannanase to improve its substrate affinity by in silico design and site-directed mutagenesis. J Ind Microbiol Biotechnol 41:693–700

Lu H, Zhang H, Shi P, Luo H, Wang Y, Yang P, Yao B (2013) A family 5 β-mannanase from the thermophilic fungus *Thielavia arenaria* XZ7 with typical thermophilic enzyme features. Appl Microbiol Biotechnol 97:8121–8128

Lu H, Luo H, Shi P, Huang H, Meng K, Yang P, Yao B (2014) A novel thermophilic endo-β-1,4-mannanase from *Aspergillus nidulans* XZ3: functional roles of carbohydrate-binding module and Thr/Ser-rich linker region. Appl Microbiol Biotechnol 98:2155–2163

Moreira LRS, Filho EXF (2008) An overview of mannan structure and mannan-degrading enzyme systems. Appl Microbiol Biotechnol 79: 165–178

Niesen FH, Berglund H, Vedadi M (2007) The use of differential scanning fluorimetry to detect ligand interactions that promote protein stability. Nat Protoc 2:2212–2221

Pham TA, Berrin JG, Record E, To KA, Sigoillot JC (2010) Hydrolysis of softwood by *Aspergillus* mannanase: role of a carbohydrate-binding module. J Biotechnol 148:163–170

Puchart V, Vrsanska M, Svoboda P, Pohl J, Ogel ZB, Biely P (2004) Purification and characterization of two forms of endo-β-1,4-mannanase from a thermotolerant fungus, *Aspergillus fumigatus* IMI 385708 (formerly *Thermomyces lanuginosus* IMI 158749). Biochim Biophys Acta 1674:239–250

Sabini E, Schubert H, Murshudov G, Wilson KS, Siika-Aho M, Penttila M (2000) The three-dimensional structure of a *Trichoderma reesei* β-mannanase from glycoside hydrolase family 5. Acta Cryst D56: 3–13

Stålbrand H, Siika-aho M, Tenkanen M, Viikari L (1993) Purification and characterization of two β-mannanases from *Trichoderma reesei*. J Biotechnol 29:229–242

Tang C, Guo J, Wu M, Zhao S, Shi H, Li J, Zhang H, Wang J (2011) Cloning and bioinformatics analysis of a novel acidophilic β-mannanase gene, Auman5A, from *Aspergillus usamii* YL-01-78. World J Microbiol Biotechnol 27:2921–2929

Tang CD, Li JF, Wei XH, Min R, Gao SJ, Wang JQ, Yin X, Wu MC (2013) Fusing a carbohydrate-binding module into the *Aspergillus usamii* β-mannanase to improve its thermostability and cellulose-binding capacity by *in silico* design. PLoS One 8:e64766

Tang CD, Guo J, Li JF, Wei XH, Hu D, Gao SJ, Yin X, Wu MC (2014) Enhancing expression level of an acidophilic β-mannanase in *Pichia pastoris* by double vector system. Ann Microbiol 64:561–569

van Zyl WH, Rose SH, Trollope K, Görgens JF (2010) Fungal β-mannanases: mannan hydrolysis, heterologous production and biotechnological applications. Process Biochem 45:1203–1213

Voutilainen SP, Murray PG, Tuohy MG, Koivula A (2010) Expression of *Talaromyces emersonii* cellobiohydrolase Cel7A in *Saccharomyces cerevisiae* and rational mutagenesis to improve its thermostability and activity. Protein Eng Des Sel 23:69–79

Wang J, Zeng D, Liu G, Wang S, Yu S (2014) Truncation of a mannanase from *Trichoderma harzianum* improves its enzymatic properties and expression efficiency in *Trichoderma reesei*. J Ind Microbiol Biotechnol 41:125–133

Xie ZH, Shi XJ (2009) Fast and almost 100% efficiency site-directed mutagenesis by the megaprimer PCR method. Prog Biochem Biophys 36:1490–1494

Xie J, Song L, Li X, Yi X, Xu H, Li J, Qiao D, Cao Y (2011) Site-directed mutagenesis and thermostability of xylanase XYNB from *Aspergillus niger* 400264. Curr Microbiol 62:242–248

Xu M, Zhang R, Liu X, Shi J, Xu Z, Rao Z (2013) Improving the acidic stability of a β-mannanase from *Bacillus subtilis* by site-directed mutagenesis. Process Biochem 48:1166–1173

Zhang Y, Ju J, Peng H, Gao F, Zhou C, Zeng Y, Xue Y, Li Y, Henrissat B, Gao GF, Ma Y (2008) Biochemical and structural characterization of the intracellular mannanase AaManA of *Alicyclobacillus acidocaldarius* reveals a novel glycoside hydrolase family belonging to clan GH-A. J Biol Chem 283:31551–31558